END
DATE
FILMED
0 81
DTIC

PR 319-125

(12) 14

K. Tayley

FINAL REPORT
ONR CONTRACT N0001477C0415
Measurement of Pair-Quasiparticle Interference
in Josephson Tunnel Junctions

(1) LEVEL II

I.   Theoretical Phase

The first summer of the contract period was spent at NBS
Boulder. Work done in collaboration with R. Peterson of NBS
Boulder was published some time ago. (Phys. Rev. B18, 1198
(1978). A copy is attached.

A successful program for applying the microscopic theory
to the computation of the time-dependent behavior of a Josephson
junction has now been developed. It was based, originally,
on one due to D. MacDonald of NBS Boulder, but extensive modifica-
tions had to be made in order to bring the computation time
and computer memory requirements down to levels that made it
possible to deal with the kinds of problems I wished to attack.

Such computations are very demanding because a junction
has a long "memory". Its behavior at some moment is dependent
on its history over a long time interval in the past. It can
be shown that the length of this memory is directly related
to the sharpness of the voltage jump that appears in the junction
current-voltage characteristic at the gap voltage. R. Harris
of NBS Boulder has pointed out that real junctions do not have
as sharp a jump as theory predicts, and this implies that their
memories are not as long as theory suggests. I investigated
this question and found that artificially shortening the theo-
retical memory does indeed lead to rounding of the jump at
the gap voltage. I found that the amount of shortening that
is required to give a reasonable rounding is in fact enough
to produce an appreciable reduction in both computation time
and computer memory requirements. This change and various
improvements in the program allowed accurate microscopic theory
computations to be made for times as long as 160T, where T
is the characteristic gap time given by Planck's constant divided
by the gap energy 2Δ. I believe that no one has done anything
close to this up to now.

At the end of this report I have appended a copy of the
article (IEEE Trans. Magnetics MAG-17, 809 (1981) that describes
my calculations, using the above program, of flux entry into
a single junction SQUID. This was the problem that this contract
was intended to study. The results bear out the prediction,
made in the proposal for this project, that at high frequencies
the simple resistively-shunted junction model is not satisfactory
for calculating this flux entry.

DTIC
SELECTED
OCT 6 1981
B

10 JUNE 1981

462342

Also appended is another article (J. Appl. Physics, accepted
for publication) on the remainder of the work that I have done
with the new program. It gives some of the details of the method
plus examples of its application. The applications include calcu-
lation of current-voltage characteristics, both with and without
the artificial "forgetting" that I mentioned earlier, and a study
of the details of the switching of a junction from the zero-
voltage to non-zero voltage state. As with the SQUID computations,
I found that the RSJ model greatly overestimates the amount of
damping that occurs.

II.   Experimental Phase

I was forced to abandon the experimental part of the project.
All of the students who were involved have left Buffalo. In
particular, one student, a Ph.D. candidate who had worked for
two years, dropped out of school for personal reasons.

III. Applications

The high-speed Josephson junction circuits that have been
investigated with the program developed in this project are
not very different from some proposed real devices, and the
quantities that have been calculated are of considerable interest
for device design. The basic finding is that the "resistively
shunted junction" model that is commonly used for device analysis
will in some cases give poor results. Even fairly sophisticated
improved versions of that model will be poor in some circumstances.

Further applications of the new program are now needed
in order to determine when it is important to use it for device
design and when the simpler models previously used are adequate.

COMPARISON OF THE MICROSCOPIC THEORY AND THE RSJ MODEL OF

JOSEPHSON TUNNELING FOR CALCULATING THE AMOUNT OF

FLUX ENTRY INTO A SINGLE-JUNCTION SQUID

Robert I. Gayley

Physics Department, State University of New York

at Buffalo

Amherst, NY 14260

Smith and Blackburn[1] and Blackburn et al[2] measured flux entry into single junction SQUIDs and found results that disagreed with their calculations, which were based on the resistively shunted junction (RSJ) model. Since this model is known to be very crude, it seems worthwhile to see if use of a more accurate theory could remove the discrepancy. Also, this system, or a more complex version of it, holds promise for use as a high speed computer element, so it is important to understand its behavior in some detail. This paper presents the first study of this SQUID using the full BCS theory of superconductivity. The results are quite different from the RSJ model predictions, but the disagreement with experiment is made worse.

The experiments dealt with a large superconducting loop of inductance L interrupted by a Josephson tunnel junction. A magnetic field, applied perpendicular to the plane of the loop, was slowly increased until a critical point was reached at which a large amount of magnetic flux would abruptly break into the loop. The measured quantity was ϕ_{enter}, which we will denote ϕ_e, the flux in the loop at the conclusion of this break-in.

The equivalent circuit for the specimen would be an inductance L in parallel with a tunnel junction of critical current I_c, energy gap 2Δ, and normal state resistance R_N and also in parallel with the junction capacitance C. All wires are taken as superconducting so that the only losses would be from the tunneling process and so that the magnetic fluxoid in the loop would be quantized in any steady state situation. In the RSJ model the tunneling is represented by a element obeying the Josephson relation $I = I_c \sin\theta$, where I is the supercurrent, and θ is the quantum mechanical phase difference across the junction, in parallel with a constant resistance R_N which represents dissipative quasiparticle tunneling. In the present work, on the other hand, the tunneling is described using Werthamer's[3] analysis of the time-dependent behavior of a junction according to the BCS theory. Within the context of that theory, this is a completely general treatment of the problem even when the voltage is time-dependent.

I have studied this system using a computer simulation which is based on the following time domain equations developed by Harris.[4]

$$I(t) = \frac{1}{2\pi} Im \left[U^*(t) \int_{-\infty}^{t} I_{qp}(t-t')U(t')dt' \right.$$
$$\left. + U(t) \int_{-\infty}^{t} I_J(t-t') U(t')dt' \right], \quad (1)$$

where

$$U(t) = \exp[-i\frac{e}{\hbar}\int_0^t V(t')dt' - \frac{1}{2} i \theta_0]. \quad (2)$$

Here I(t) is the tunneling current at time t in terms of the junction voltage V(t). The constant θ_0 is the

t = 0 value of the phase difference across the junction, and it is assumed that V is zero for t < 0. The kernels $I_{qp}(t)$ and $I_J(t)$ are zero for negative argument. For identical superconductors at absolute zero and for $t \geq 0$ they are

$$I_{qp}(t) = -2\pi(\hbar/eR_N)\delta'(t)$$
$$+ \frac{2\pi^2\Delta^2}{\hbar eR_N} J_1 \left(\frac{t\Delta}{\hbar}\right) Y_1 \left(\frac{t\Delta}{\hbar}\right) \quad (3)$$

and

$$I_J(t) = \frac{2\pi^2\Delta^2}{\hbar eR_N} J_0 \left(\frac{t\Delta}{\hbar}\right) Y_0 \left(\frac{t\Delta}{\hbar}\right), \quad (4)$$

where J_n and Y_n are the nth-order Bessel functions of the first and second kind, respectively. The details of the method are given elsewhere,[5] but one unusual feature needs to be explained again here. I have introduced an artificial "memory reduction" into the kernels $I_{qp}(t)$ and $I_J(t)$ by multiplying each Bessel function by $\exp(-t^2/2A\tau^2)$, where $\tau = h/2\Delta$ and A is a constant which for tin junctions is taken to be 50. In addition, the Bessel functions were set equal to zero whenever the t in their arguments exceeded 20τ. Reference 5 shows that these modifications change the results by no more than a few percent (and the change may actually be an improvement for real junctions). Their effect is to artificially introduce a small amount of energy gap rounding, and the constant A was chosen to give the amount of rounding appropriate for tin. These changes greatly reduce the demands on the computer whenever it is necessary to follow the junction behavior for a long period of time, and this makes calculations feasible which otherwise would be impractical.

The BCS relation between I_c, R_N and Δ was assumed to hold, so the only parameters that can vary from SQUID to SQUID are L, I_c, R_N, and C. They will be expressed in terms of the dimensionless parameters $\beta \equiv \sqrt{LC}/R_N C$ and $\gamma \equiv LI_c/\phi_0$ where ϕ_0 is the flux quantum. β is the familiar damping constant of the LCR oscillator, and γ is the number of flux quanta produced by a current I_c circulating in the loop. The basic junction parameter used in reference 5, $R_N C/\tau$, can be found from $R_N C/\tau = 2\gamma/\pi\beta^2$.

One result of the computations is the dependence of ϕ_e on γ and β. This is shown in Fig. 1, where the dimensionless quantity $\phi_e/\gamma\phi_0$ is plotted against β. Only cases for which $\phi_e/\gamma\phi_0$ was less than unity are shown. For larger values, the results will tend to be erratic and very sensitive to initial conditions.[6] The figure shows two RSJ points. They are for $\gamma = 500$ but more closely resemble the BCS results for $\gamma = 50$.
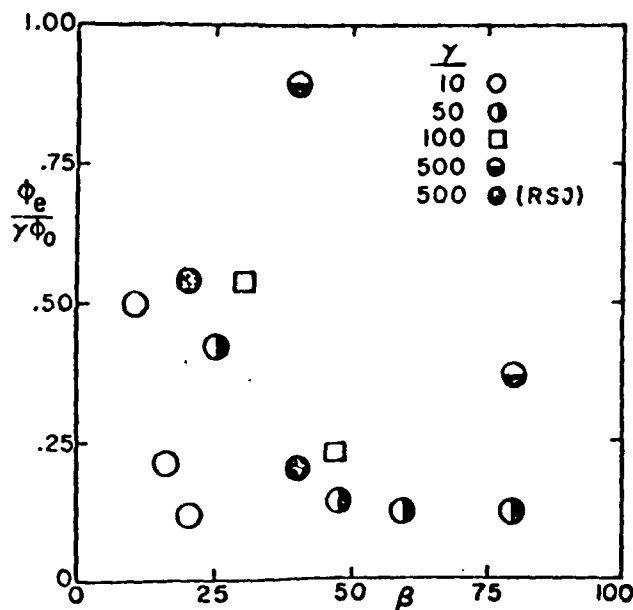
Figure 1. Dependence of the amount of flux ϕ_e entering the SQUID on the damping parameter β. $\gamma\phi_o$ is LI_c. All of the points except the solid circles were computed using the BCS theory. The solid circles were taken from Fig. 2 of reference 1.

To shift one of these points to the BCS value would require increasing the β value used in the graph, which could be regarded as decreasing the effective resistance used in calculating β. On the other hand, if one calculates β from R_N, then the correct ϕ_e could be obtained by using a larger "effective R_N" in the computer simulation, which would reduce the amount of damping and give a larger ϕ_e. In this sense, the original RSJ calculation overestimates the amount of damping.

In addition, some qualitative conclusions from the RSJ analysis do not apply in the BCS case. Smith and Blackburn[1] found an expression for a quantity $\beta_c(\gamma)$ which gave the minimum β such that ϕ_e was one quantum. This same β_c gave a universal curve when ϕ_e/γ was plotted against β/β_c. There seems to be no equivalent quantity for the BCS results. In fact, for at least one case ($\gamma=50$) there seems to be no sensible value of β that will restrict ϕ_e to one quantum. In Fig. 1, $\phi_e/\gamma\phi_o$ seems to be approaching a limit of about 0.1 ($\phi_e = 5\phi_o$). Even with the totally unrealistic value of β of 5600 (not shown) ϕ_e is still $5\phi_o$.

An interesting feature was observed for this case of $\gamma=50, \beta = 5600$. The time derivative of the flux in the loop became slightly negative briefly when ϕ_e was $1.25\phi_o$. It then became positive again, and ϕ_e continued to increase to $5.3\phi_o$. This is quite inexplicable by the RSJ model (even if modified to let the resistance be voltage dependent). In that picture, once the flux has started to decrease in the potential energy well corresponding to a particular number of quanta the system will be trapped in that well.

Blackburn et al[2] proposed that the principle

source of disagreement between their measurements and their RSJ calculation was the effects of finite quasiparticle lifetimes in the metal films of the junctions. I have not actually calculated the behavior of Smith and Blackburn's specimen, which had $\gamma = 5 \times 10^5$. Even with memory reduction, such a large value of γ makes the computer simulation impractical. However, because of the universal curve for ϕ_e/γ found by them, there is no reason to doubt that for this case the BCS and RSJ calculations will differ in the same general way as they do for smaller γ. In other words, it is clear that the BCS calculation will give greater disagreement with the experiment, and it seems unlikely that finite lifetime effects can be responsible.

For device considerations it is also of interest to determine the time required for flux entry in the SQUID. There is an initial period of very slow change, until the flux is near one quantum. For the rest of the time the average junction voltage is close to the gap voltage, and flux enters at the corresponding rate of $2\phi_o/\tau$. The time for the first quantum to enter, which I will call t_1, depends only on R_NC for the range of parameters studied. As Fig. 2 shows, t_1/τ approaches a minimum value of 4.7 for small R_NC. For larger R_NC, it becomes roughly proportional to $(R_NC/\nu)^{\frac{1}{2}}$.
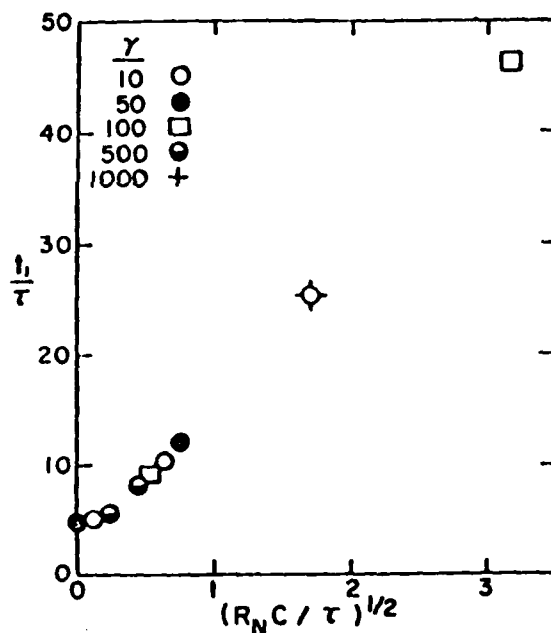

Figure 2. Dependence on device parameters of the time t_1 for the first quantum of flux to enter the SQUID, according to the BCS theory. When t_1/τ is plotted against $(R_NC/\tau)^{\frac{1}{2}}$, a universal curve results that is roughly linear for larger R_NC. (The β values for each point can be computed from $\beta = (2\gamma\tau/\pi R_NC)^{\frac{1}{2}}$).

The RSJ model gives similar behavior, except that the average voltage falls appreciably below the gap value in the later stages of flux entry. As an example, our own unpublished RSJ calculations give the following results for $\gamma = 120$, $\beta = 5$: t_1 is 120τ, and the total time to reach the final value of $\phi_e = 93\phi_o$ is 238τ, so

that $d\phi/dt$ averaged $.8\phi_o/\tau$ after t_1. The
BCS values are: $t_1 = 26\tau$, $\phi_e = 124\phi_o$, total time
$= 88\tau$, and the average rate after t_1 is $2.0\phi_o/\tau$. Smith
and Blackburn did not measure these times (they
are, of course, extremely short), so it is not pos-
sible to compare theory and experiment. In any
case, we again see that the RSJ model overestimates
the damping.

In summary, the simple constant resistance RSJ
model gives poor results for flux entry into a
single-junction SQUID and is not suitable for quanti-
tative comparison with experiment. (A modified RSJ
model in which a kind of energy gap is introduced
by giving the resistance a suitable voltage de-
pendence may work better, but computer simulation
of single junction switching[5] shows that even this
is not necessarily satisfactory.) The predictions
of the BCS theory do not agree with experiment.
The reason for this is not known.

1. H.J.T. Smith and J.A. Blackburn, Phys. Rev.
   B12, 940 (1975).

2. J.A. Blackburn, H.J.T. Smith, and V. Keith,
   Phys. Rev. B15, 4211 (1977).

3. N.R. Werthamer, Phys. Rev. 147, 255 (1966).

4. R.E. Harris, Phys. Rev. B13, 3818 (1976) and
   J. Appl. Phys. 48, 5188 (1977).

5. R.I. Gayley, J. Appl. Phys., to be pub-
   lished.

6. T.C. Wang and R.I. Gayley, Phys. Rev. B15,
   3401 (1977).

Josephson tunnel junction time-dependence
calculations based on the BCS theory

Robert I. Gayley

Department of Physics
State University of New York at Buffalo,
Amherst, New York 14260

ABSTRACT

The feasibility and the importance of using the full BCS theory for numerical calculations of the time-dependent behavior of a Josephson tunnel junction is examined by investigating switching from the zero to the finite voltage state. The calculation can be done, but only if the RC time constant is not too long. The results differ appreciably from those obtained with the crude but frequently used "resistively shunted junction" model. Artificial rounding of the energy gap edge, in the form of "memory reduction", is introduced and shown to reduce computational difficulties appreciably without significantly altering any results. This should make many more situations amenable to accurate digital simulation.

I. Introduction

The qualitative behavior of a Josephson tunnel junction can be understood using the very simple "resistively shunted junction" (RSJ) model, but accurate calculations, particularly at high frequencies or where damping is important, require a more detailed analysis. This paper presents the start of an investigation of the consequences of applying the BCS microscopic theory to time-dependent problems. We will see that in some instances the quantitative results are quite different from those obtained with the RSJ model.

The analysis has been done by computer simulation, and the method used will be discussed in the following section. In addition, some computations using a modified form of the theory which gives nearly the same results but greatly reduced computation cost will be described.

II. Method of Calculation

The BCS theory was used to calculate junction behavior by applying Harris'[1] time domain formulation of Werthamer's[2] analysis of junction dynamics. The basic relation gives the tunneling current I at time t in terms of the voltage V at all times up to and including t. In Harris' notation it is

$$I(t) = \frac{1}{2\pi} \, \text{Im} \, [U^*(t) \int_{-\infty}^{\infty} I_{qp}(t-t')U(t')dt'$$

$$+U(t)\int_{-\infty}^{\infty} I_J(t-t')U(t')dt'], \tag{1a}$$

where

$$U(t) = \exp\,[-i\,\frac{e}{\hbar}\int_{0}^{t} V(t')dt' + \frac{1}{2}\,i\,\phi_0]. \tag{1b}$$

The constant ϕ_o is the $t = 0$ value of the phase difference across the junction, and it is assumed that V is zero for $t < 0$. Equation (1a) appears to require knowledge of V for all times in the future as well as the past, but this is not so since the kernels $I_{qp}(t)$ and $I_J(t)$ are zero for negative argument. For identical superconductors at absolute zero and for $t \geqslant 0$ they are

$$I_{qp}(t) = -2\pi \ (\hbar/eR_N)\delta'(t)$$

$$+ \frac{2\pi^2\Delta^2}{\hbar eR_N} \ J_1 \ (\frac{t\Delta}{\hbar}) \ \ Y_1(\frac{t\Delta}{\hbar})$$

$$I_J(t) \ = \frac{2\pi^2\Delta^2}{\hbar eR_N} \ J_0 \ (\frac{t\Delta}{\hbar}) \ Y_0(\frac{t\Delta}{\hbar}). \tag{2}$$

Here R_N is the normal state tunneling resistance of the junction, 2Δ is the energy gap, and J_n and Y_n are the nth-order Bessel functions of the first and second kind, respectively.

This represents an exact microscopic description, based on the BCS theory, with the following limitations: (1) Only identical superconductors at absolute zero are considered here; (2) The junction must be small so that spatial variations can be ignored; (3) No nonequilibrium or quasiparticle lifetime effects are included; (4) Energy gap anisotropy is ignored; (5) No losses in the superconducting metal are included.

A second equation relating I(t) and V(t) will be given by the specific circuit being considered. If the initial values ϕ_o and V(0) are given, the two equations can be integrated numerically to give I(t) and V(t). (The junction capacitance C is treated as part of the external circuit.)

Harris used this approach to find the effect of applying a voltage pulse,[1] to examine the switching of a junction having an external load resistance,[3] and to investigate the small, sinusoidal voltage limit.[4] McDonald, Johnson, and Harris[5] analyzed a few current-biased cases to check their frequency domain calculations of current-voltage characteristics. Noting that Eq. (1a) requires V at time t to determine I at the same time, and that (1a) is nonlinear in V because of the form of U, they used an iteration scheme that starts with a guessed value for V. In the present calculations a simpler procedure has been used. Equation (1b) was expanded in a power series to first order in the quantity $(\Delta t/\tau)(V_{new}-V_{old})/V_{old}$, where τ is $h/2\Delta$. This is of order $(\Delta t/\tau)^2$, which is the order to which all approximations were made. Equation (1a) is thereby linearized and can be solved simultaneously with the linear circuit equation.

The accuracy of the results was investigated by comparing computations done with and without double precision arithmetic, by varying the time step size, and, where possible, by comparing with results of frequency-domain calculations. These tests indicated that all results presented here are good to 2 percent or better.

Anyone interested in further details of the computation method is urged to contact the author directly. However, it is important to note that the form of Eqs. (1) and (2) make the calculation very demanding. First of all, the kernels in Eq. (1) decay as t^{-1}, which is very slow. The integrals in Eq. (1a) are of the form of convolutions and must be done all over again for each time step. This means that the computation time will increase as t^2. It also means that every

value of I_{qp}, I_J, and the real imaginary parts of U must be remembered. Depending on the computing facilities available, either the computing time or the memory requirement can limit the maximum t that can be considered.

These difficulties are compounded by two facts. One is that typical junctions have RC time constants of the order of 10τ or more. The other is that τ, a characteristic time for a junction, is of the order of picoseconds, which is very short compared to the time scale of most measurements. The second fact means that we sometimes cannot numerically duplicate the procedure of an experiment, such as the determination of a current-voltage characteristic, but must start with unphysical initial conditions. The first fact means that the inevitable transients produced by this will require many τ's to die away. As an example, consider the I-V characteristic for $R_N C = 10\tau$ which will be presented below. Each point was obtained from a separate calculation. The time step necessary to get good results was $.02\tau$, and it was necessary to compute for 80τ in order to determine the average voltage to within less than 1% of its limiting value. Thus, 4000 time steps were required, as well as the storage of four 4000-element arrays. It is therefore not surprising that with the existing computer program it was not feasible to work with larger values of $R_N C$.

There are various steps which can be taken to reduce these difficulties. One is to improve the approximations made in the numerical method and thereby allow longer time steps to be used. This is now being worked on.

Another modification is based on the fact that the kernels
I_J and I_{qp} do eventually become negligibly small. For large
enough t-t´ they can be set equal to zero. Beyond this point the
computing time goes as t instead of t^2, and the size of the
arrays that must be remembered does not increase. In practice
this has not been found helpful except when combined with
another change, a reduction in the length of the junction's
"memory".

"Memory" refers to the fact that I at time t depends
on V at all previous times. The slow fall off of the kernels
gives a very long memory. Harris[3] has pointed out that the
length of the memory is directly related to the sharpness
of the rise in current seen in the I-V characteristic at the
gap voltage. The rise exhibited by real junctions is never as
sharp as is predicted by the BCS theory. Harris suggested
that this means that the memory of real junctions is shorter
than predicted, or in other words, the real kernels fall off
more rapidly than as t^{-1}. Perhaps a more detailed theory,
including such complications as gap anisotropy, would give
modified kernels leading to a shorter memory and thereby
simplifying numerical computations.

In lieu of such a more detailed theory, the consequences
of a phenomenological reduction in memory have been investigated,
and the results are rather encouraging. In some of the cal-
culations to be described below, each of the Bessel functions
in Eq. (2) was multiplied by exp $(-t^2/2A\tau^2)$. The constant A
was chosen to be 50, which altered the I-V characteristic by a few

percent, giving a rounding that matched fairly closely what was observed in tin tunnel junctions.[6] Instantaneous current and voltage values were also changed by only a few percent, and usually less than two percent, which for most practical purposes is not significant. This allows one to hope that a modification based on physical grounds would also not alter the detailed time dependence by a large amount and that the Werthamer theory as well as the phenomenological modification introduced here will not disagree substantially with a more complete treatment. In any case, the memory reduction used does not degrade the results significantly, and it has the great advantage that it allows the kernels to be replaced by their limiting value of zero at much smaller t. As explained earlier, this greatly reduces the demands made on the computer. For $R_N C = 10\,\tau$ and $A = 50$, this replacement could be made at $t = 20\,\tau$.

Besides giving a more realistic I-V characteristic, this memory reduction will be shown to reduce and broaden the Riedel peak,[7] which is what one would expect. A side effect is a reduction in I_c, the maximum zero-voltage supercurrent. It is not known whether this is physically correct or not, but since the change is only .004% for the A value used, it is of no practical consequence.

One goal of this work is to examine the accuracy of the RSJ model by comparing its predictions with those of the BCS theory. The basic RSJ model treats the junction as a resistor R, equal to the normal state resistance R_N, in parallel with a capacitor C and also in parallel with an element obeying the equation $I = I_c \sin\phi$, where ϕ is the superconducting phase difference across the junction. There is nothing corresponding to an energy gap in this picture, and so of course the resulting I-V characteristic shows no structure at the gap.

There is an extensive literature of calculations of junction behavior with this model, and many features can be understood qualitatively in this way. The simplest and probably most important improvement that can be made in the model is to let R be voltage dependent. This can obviously give a fairly realistic looking I-V characteristic if R(V) is chosen appropriately, and it probably gives greatly improved results for any calculation. Results obtained with both the basic RSJ model and the variable resistance version will be presented. In the latter, R(V) was chosen so that I = V/R would fit our experimental I-V curves for tin junctions[6]. These junctions had an $R_N C/\tau$ value of about 60, rather than the 10 that is used in most of these calculations. However, the I-V curve is not expected to change significantly in this particular range of $R_N C/\tau$. From the description of the equivalent circuit, one can see that the equation that replaces Eq. (1) is

$$I = I_c \sin\phi + V/R, \tag{3a}$$

where

$$\phi = \frac{2e}{\hbar} \int_0^t V(t') \, dt' + \phi_0. \tag{3b}$$

The junction capacitance is treated as part of the external circuit, as before. Equations (3) together with the appropriate circuit equation can be numerically integrated in a straight-forward way. The "memory" or dependence on past voltage is of a simple nature in this case and does not lead to the computational difficulties found with the BCS theory.

All of the results will be expressed in normalized units. Current is divided by the critical current $I_c = \pi\Delta/2eR_N$, and voltage by the gap voltage $V_g = 2\Delta/e$. The unit of time is $\tau = h/2\Delta$. As before, R_N is the junction normal state resistance and 2Δ is the energy gap at absolute zero. The only adjustable parameter that can distinguish one junction from another is the dimensionless RC time constant $R_N C/\tau$, which is independent of junction area. It is proportional to the oxide barrier's dielectric constant to thickness ratio and inversely proportional to the maximum supercurrent per unit area. In practice, for a given material, the former varies little from junction to junction, but the latter can sometimes vary over several orders of magnitude. For tin-tin oxide-tin junctions $R_N C/\tau = 10$ would correspond to the reasonable supercurrent density value of about 10^2 A/cm^2. This is the value used in this paper, but it should be borne in mind that many aspects of a junction's behavior depend rather strongly on this parameter.

III. Applications

A. Current-voltage characteristics

Since voltage and frequency are directly proportional for a Josephson junction, the natural approach to finding the I-V curves from Werthamer's analysis is to work in the frequency domain. This has been done by McDonald et.al.[4] and by Schlup.[8] The time domain formulation is used to compute I-V characteristics here in order to check that the program is correct and to investigate the phenomenological memory reduction that was described in the previous section.

The circuit in this case is a Josephson junction in parallel with a capacitor C and the combination in series with a constant current source. The tunneling current, the displacement current, and the voltage will vary rapidly and sometimes with large amplitude. However, the discussion here will be limited to the average voltage, since this is what is measured.

With $R_N C/\tau = 10$ a time step of $.02\tau$ gave instantaneous current and voltage values to about 1 percent or better. The initial value of phase, ϕ_o, was chosen so that the initial tunneling current equalled the current I_{dc} from the constant current source. The initial voltage was usually taken to be the gap value. This is unphysical since the formalism assumes $V = 0$ for all $t < 0$. This led to rather violent transient behavior, and so the computation was carried out to large enough t so that the average voltage no longer changed. (Even though it required allowing the transients to die out, this scheme seemed to require less computation time than would others that could be imagined.) Then the process was repeated with a new value of I_{dc}. In order to check that the maximum zero-voltage current had the correct value, some computations with I_{dc} in the neighborhood of I_c were given an initial voltage of zero. For $I_{dc} \leq I_c$ the voltage remained zero, as it should. For $I_{dc} \leq I_c$ but initial voltage equal to the gap value, the average voltage was nonzero.

The result is shown by the circles in Figure 1. The shape of this curve is consistent with the frequency domain results of McDonald et. al.[4] and of Schlup.[8] The accuracy of the voltage values is believed to be 1%. Note that the

sharp current rise at the gap voltage has a voltage width
of 2%, so it is not possible to be positive that this width is
real. However, the small foot on the low voltage side of the
current rise is real. The dashed line is drawn from a point
computed for $I_{dc}/I_c = 10$ and has a slope corresponding closely
to R_N.

The solid line is taken from I-V curves measured on our
high-quality tin tunnel junctions.[6] Notice that the current
rise at the gap voltage is not as sharp as theory predicts.
For tin, there is evidence that this is due to the large variation
in the size of the gap for different crystallographic directions.[9,10]
However, it seems that junctions of other, less anisotropic,
materials show comparable rounding. For the present phenomeno-
logical approach it is assumed that the physical cause of the
rounding is not important. At worst, the memory reduction introduced
does not produce a large change in the results, and, at best it may
actually improve them, just as it improves the I-V curve.

The crosses show the change produced by memory reduction.
The parameter A was chosen to be 50 by requiring the voltage
value at $I_{dc}/I_c = 1.0$ to match that observed in the tin tunnel
junctions. The result is very plausible, being closer to the
experimental curve than is the unmodified curve. It confirms
Harris' statement that gap rounding will result from memory
reduction.

B. Constant-voltage coefficients

When the junction voltage is constant, Josephson[11] showed that the tunneling current can be written

$$I(V,T) = I_{J1}(V,T) \sin\phi + I_{J2}(V,T) \cos\phi + I_{qp}(V,T), \quad (4)$$

where T is the absolute temperature and the notation is that used by Harris.[12] In most situations the voltage will not be constant because typical junction resistances, of the order of an ohm, are much smaller than usual source impedances. On the other hand, a typical RC time constant of the order of 10τ keeps the voltage from varying rapidly in a time interval τ.

Therefore, there may be situations in which Eq. (4) will give fairly good results. It gives the basic RSJ model if one sets $I_{J1} = I_c$, $I_{J2} = 0$, and $I_{qp} = V/R_N$. Obvious improvements would be to give I_{J1}, I_{J2}, and I_{qp} the voltage dependences predicted by theory. Even then, however, the model is strictly correct only for constant voltage. There seems to be no way to estimate its precision except by comparison with experiment or with the full time-dependent theory. In this paper this process of comparison will be begun by examining the RSJ model and the modification in which I_{qp} has the voltage dependence suggested by experiment.

The coefficients of Eq. (4) were computed for $T = 0$ using the time-dependent program described earlier. This serves as another check on the program and also allows determination of the effect of memory reduction on these coefficients.

The circuit equation for this case is simply the statement that the voltage is constant. The junction capacitance plays no role. In the program, the terms of Eq. (4) were not identifiable, so they could not be computed directly. Instead, the voltage was chosen and the computation was begun with I and ϕ_o set to zero. The effect of this is as if a voltage step function were applied at $t = 0$. The program was run until the transients died out. (A time step of $.01\tau$ was found to be suitable, so the computation could be carried out to $t = 40\tau$.) Then, from the I and ϕ values at three t's the three coefficients of Eq. (4) were determined. This process was repeated for each voltage.

For the unmodified BCS calculation, it was not feasible to get accurate results in the region within ±5% of the gap voltage since there the transients take too long to die out. Of course, some such difficulty is inevitable with any method because of the singularity (the "Riedel singularity"[7]) in I_{J1} at the gap voltage. Outside of this region the results agree with standard calculations such as those by Harris,[12] whose curves are reproduced as lines in Fig. 2.

The points in Fig. 2 show the changes produced by memory reduction, with A = 50 as before. The Riedel peak is broadened and reduced, and the abrupt jumps in I_{J2} and I_{qp} are broadened. These are the kind of alterations one would expect from a physical gap-rounding mechanism, and this lends support to the idea that the memory reduction introduced in this paper may actually improve the agreement between theory and experiment, not only for I-V curve measurement, but for other cases as well.

C. Switching

This section deals with switching of a junction from the zero voltage to the finite voltage state by a constant current source. This was chosen because it is of practical interest, it can be treated in a fairly realistic way, and it is a case where the RSJ model gives rather bad quantitative results.

The circuit is the same as for the I-V curve calculation. The initial conditions are V = 0 and ϕ_0 such that $I = I_c$. For the results presented here I_{dc} was taken to be 1.001 I_c. These are quite reasonable initial conditions. One can imagine that for the time interval $-\infty < t < 0$ the applied current was

exactly I_c and the voltage remained zero. Then at t = 0 a small increase in current caused switching to begin. This could correspond to a real experiment and should show the true time dependence of a junction being used as a switch, except for certain approximations that have been made in the treatment of the circuit. The switching will turn out to be quite fast, so a true constant current source would be hard to achieve. Also, radiation will occur, but it is not included in the equations. The latter is not likely to be of any consequence to the switching, but the former may well be, depending on the specific circuit. The present calculation will exhibit the behavior that is intrinsic to the junction itself, and there would be no particular difficulty associated with repeating the calculation with a modified external circuit.

The line labeled "BCS" in Fig. 3(a) shows what happens for $R_N C = 10\tau$. The other line shows the RSJ result.

Note that while the two calculations give qualitatively similar results, the details are quite different.

One inevitable failing of the RSJ model is that it gives the wrong final voltage because it does not give the correct resistance near $I = I_c$. This is probably of no particular concern. The switching time is likely to be what one needs to predict. For this, the RSJ model fails in two ways. First, it gives a longer delay before the onset of the rapid voltage rise. Second, it gives a more or less exponential approach to the final voltage, whereas the BCS calculation shows a steeper, nearly linear rise. For example, the RSJ case rises from 10%

of its final voltage to 90% in a time internal of 20τ, while
the BCS case rises from 10% of _its_ final voltage to 90% in
only 11τ. The BCS result also differs from the RSJ in that
the voltage shows an overshoot at the end of the rapid rise.

Calculations using a voltage-dependent resistance in the
RSJ model give much better agreement with BCS theory, as shown
in Fig. 3(b). For this calculation, the junction resistance
is very large until the voltage gets very close to the gap
value. Therefore, during most of the switching period the
current is nearly all supercurrent ($I_c \sin\phi$) or displacement
current through the capacitor. Apparently, much the same thing
is true for the BCS case. When the rapid rise begins, the RSJ cal-
culation has the voltage rising exponentially toward the very
large value that the high resistance requires. When the voltage
is approximately the gap value, the resistance drops rapidly,
sharply cutting off the rapid voltage rise. This gives a fairly
linear portion during that rise. The overshoot is still
not reproduced, however.

A similar comparison was carried out by Harris[3] for $R_N C/\tau$ = 27.
He considered the switching of a junction that had an external
load resistor, so the calculations cannot be compared directly,
but the qualitative conclusions are the same.

The important role played by junction capacitance can
be seen by comparing Fig. 3 with 4, which shows the $R_N C$ = 0.1 τ
case. The switching is much faster and the voltage oscillations
are greatly enlarged in the latter. Again, the simple RSJ
model (not shown) is in error. It gives the first peak at
7.9τ instead of 3.3τ and 1.2τ instead of .45τ for the oscillation
period. More surprisingly, the variable resistance case,
shown by dots, is also not very successful. The explanation

for the disagreement is an interesting lesson in the hazard of thinking in terms of Eq. (4). As the switching begins, V starts to change. dV/dt is very small but not zero (and it is about 100 times larger than for $R_N C/\tau = 10$), and this leads to a small additional contribution to the tunneling current besides what one would expect from Eq. (4). In fact, in the early moments the tunneling current rises slightly above I_c. Over a period of time, the cumulative effect of this additional tunneling current and the corresponding decrease in the displacement current slows the voltage rise enough to produce the delay in switching compared to the variable resistance RSJ model that Fig. 4 shows.

These calculations were repeated with memory reduction. (The parameter A was set to 50, and the kernels were cut off for t in their arguments of 20τ.) The results were nearly identical to the originals, except for a slight shift along the time axis. For $R_N C = 10\tau$, in the vicinity of the peak at 33τ, the shift was $.34\tau$. For $R_N C = 0.1\tau$, around the peaks near 3τ, the shift was $.05\tau$. It is unlikely that these differences would be of any practical consequence, so it seems sensible to use memory reduction for any further computations of this kind.

In summary, one can see that the RSJ model gives incorrect numbers and does not really give the right shape for the voltage-time curve. Simply letting R vary with V can remove most of the discrepancies for an $R_N C/\tau$ of 10 but not for 0.1. Further work is needed to more clearly delineate the extent to which models based on Eqs. (4) can reproduce the predictions of the full time-dependent calculation.

VI.   SUMMARY

One conclusion that can be drawn from this work is that calculations of the time-dependent behavior of a junction using the full BCS theory are more feasible than one might at first suppose, particularly if "memory reduction" is accepted. This is fortunate because as work proceeds on high-speed devices using Josephson junctions, it seems likely that it will be necessary to turn more and more to this approach for accurate predictions.   With regard to memory reduction, a substantial

amount does not change the results by much, and these changed
results are plausible and perhaps even closer to reality than
the unmodified case is.

As is certainly not surprising, the simple RSJ model is
shown to be defective if quantitative results are desired.
Another paper,[13] dealing with single-junction SQUIDs, shows this
even more dramatically. It deals with flux entry into such
SQUIDs and shows that, for some values of the relevant parameters,
the simple RSJ model is totally unsatisfactory.

Finally, calculations such as these can add new insight
to our understanding of junction dynamics. Equation (1) does
not lend itself readily to physical interpretation, and there
are undoubtedly consequences which have not yet been recognized.
A minor example of this is the overshoot that occurs in the
switching problem for $R_N C = 10\tau$, and more interesting examples
may well arise as work continues.

VII.   ACKNOWLEDGEMENTS

REFERENCES

1. R.E. Harris, Phys. Rev. B $\underline{13}$, 3818 (1976).

2. N.R. Werthamer, Phys. Rev. $\underline{147}$, 255 (1966).

3. R.E. Harris, J. Appl. Phys. $\underline{48}$, 588 (1977).

4. R.E. Harris, Phys. Rev. B $\underline{11}$, 3329 (1975).

5. D.G. McDonald, E.G. Johnson, and R.E. Harris, Phys. Rev. B $\underline{13}$, 1028 (1976).

6. S. Paley, J. Wilson, and R.I. Gayley, Phys. Lett. $\underline{41A}$, 311 (1972).

7. E. Riedel, Z. Naturforsch. $\underline{19a}$, 1634 (1964).

8. W.A. Schlup, Phys. Rev. B $\underline{18}$, 6132 (1978).

9. N.V. Zavaritskii, Zh. Eksp. Teor. Fiz. $\underline{39}$, 7 (1960).

10. S.A. Buckner, T.F. Finnegan, and D.N. Langenberg, Phys. Rev. Lett. $\underline{28}$, 150 (1972).

11. B.D. Josephson, Phys. Lett. $\underline{1}$, 251 (1962).

12. R.E. Harris, Phys. Rev. B $\underline{10}$, 84 (1974).

13. R.I. Gayley, submitted to the IEEE Transactions on Magnetics.(To be presented at the 1980 Applied Superconductivity Conference.)

14. For a discussion of this topic, see D.N. Langenberg, Rev. Phys. Appl. $\underline{9}$, 35 (1974).

FIGURE CAPTIONS

Figure 1   Current-voltage characteristic for a Josephson

tunnel junction with a constant current source.

The line shows a measured characteristic. The

circles are calculated from the BCS theory with

$R_N C = 10\tau$. The crosses were obtained by including

memory reduction (see text) with $A = 50$. The

dashed line shows the normal state result.

Figure 2   Effect of memory reduction on the coefficients in

the constant voltage tunneling current equation

(Eq. (4) of text). The solid lines, taken from

ref. 12, are the predictions of the BCS theory.

The points show the effect of memory reduction

with the parameter A set equal to 50. Note the

rounding of the discontinuities in I_{J2} and I_{qp}

and the fact that the singularity in I_{J1} is

replaced by a finite, broadened peak.

Figure 3   Normalized voltage versus normalized time for

switching to the finite voltage state for

$R_N C = 10\tau$ and for a constant current of $1.001\ I_c$.

(a) Predictions of the BCS theory and the RSJ model.

(b) Prediction of the RSJ model with voltage-

dependent resistance. The dashed line indicates

the BCS result from (a) for the longer times where

it differs. The two are indistinguishable on this

scale for t/τ less than about 27, with the oscil-

lations matching precisely.

Figure Captions (continued)

Figure 4   Switching for $R_NC = 0.1\tau$. The RSJ model with

voltage-dependent resistance, shown by the dots,

does not agree as well with the BCS prediction as

was the case for $R_NC = 10\tau$ (Fig. 3). However it

is still much better than the constant resistance

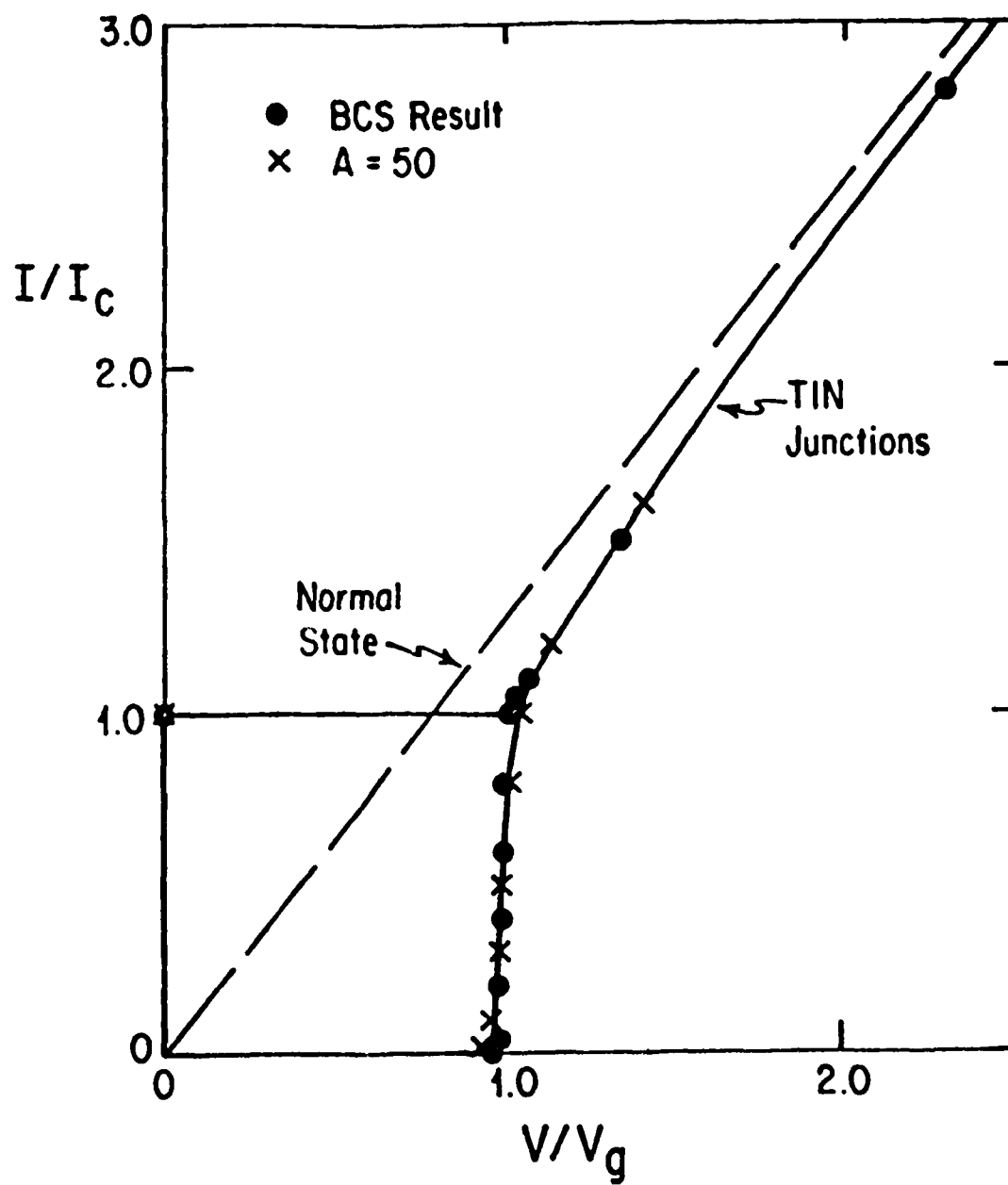version (not shown), which does not reach the first
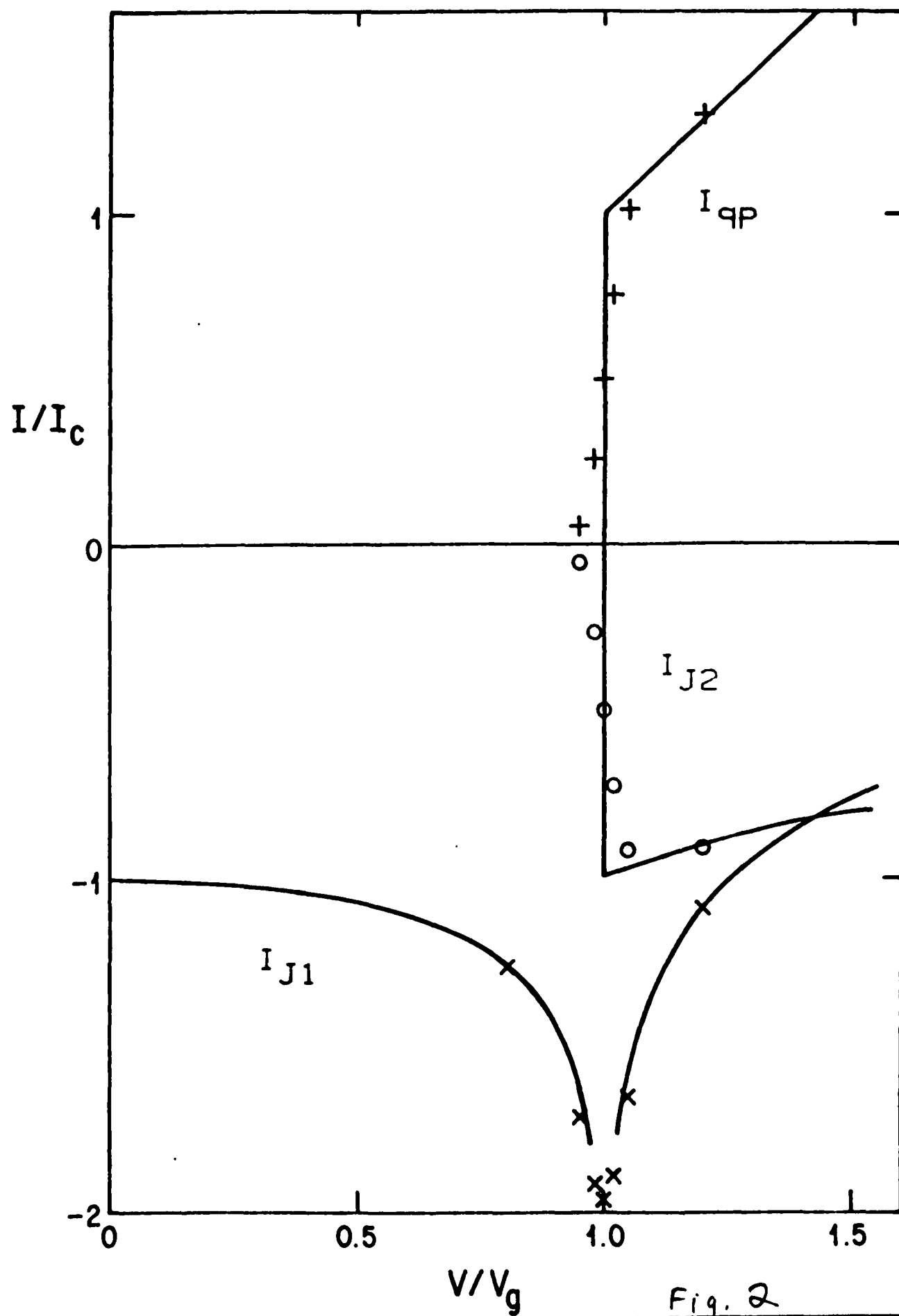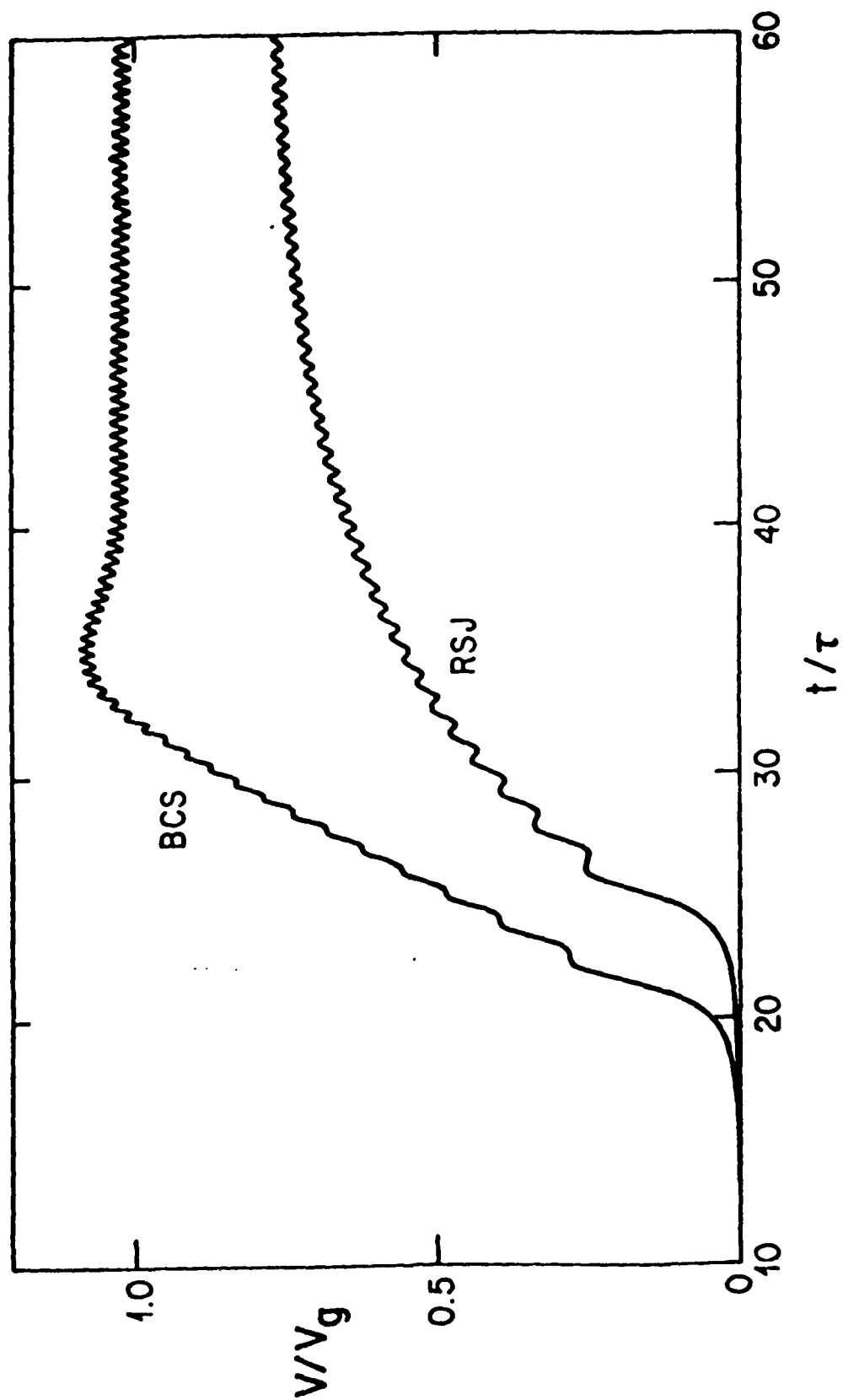
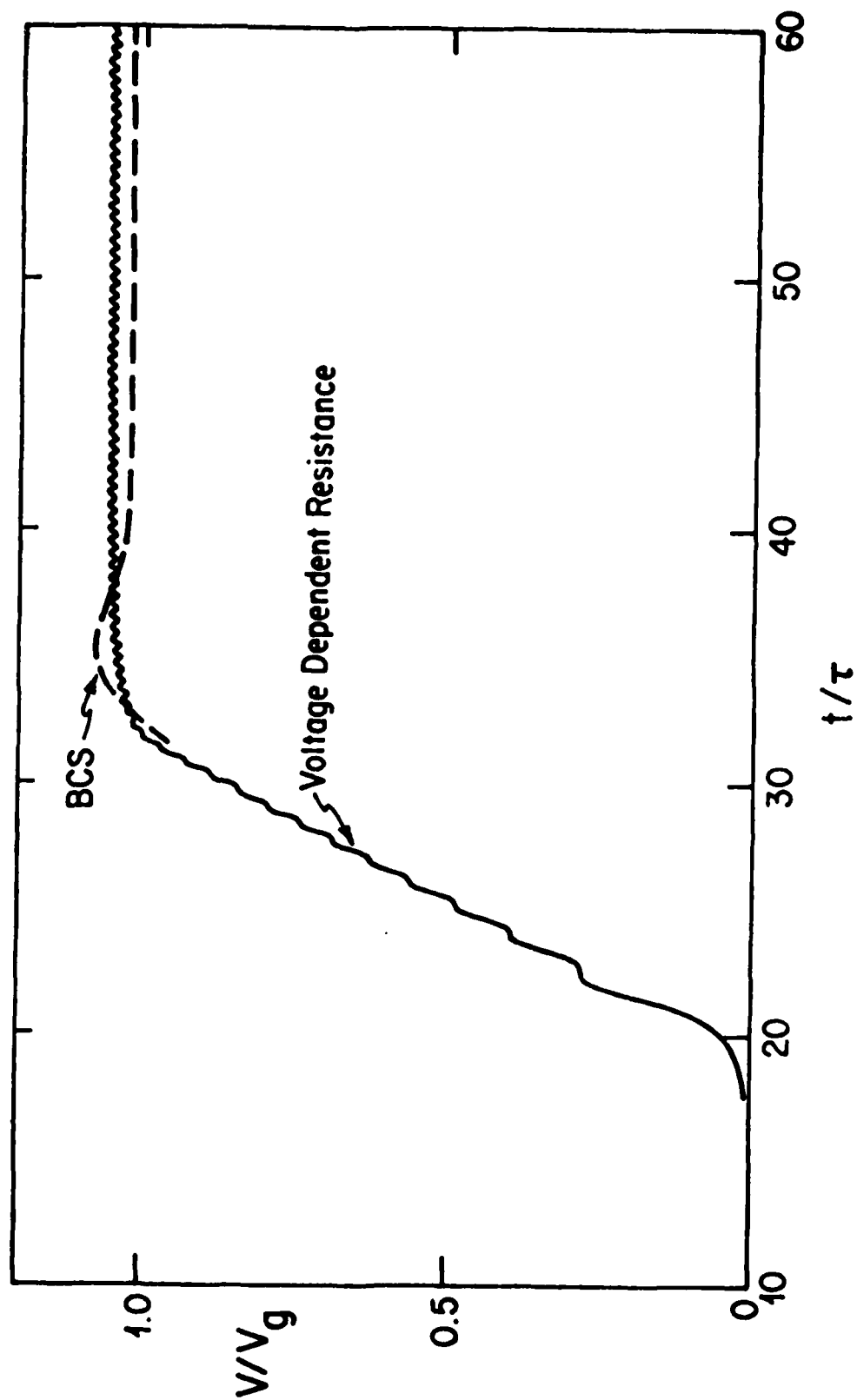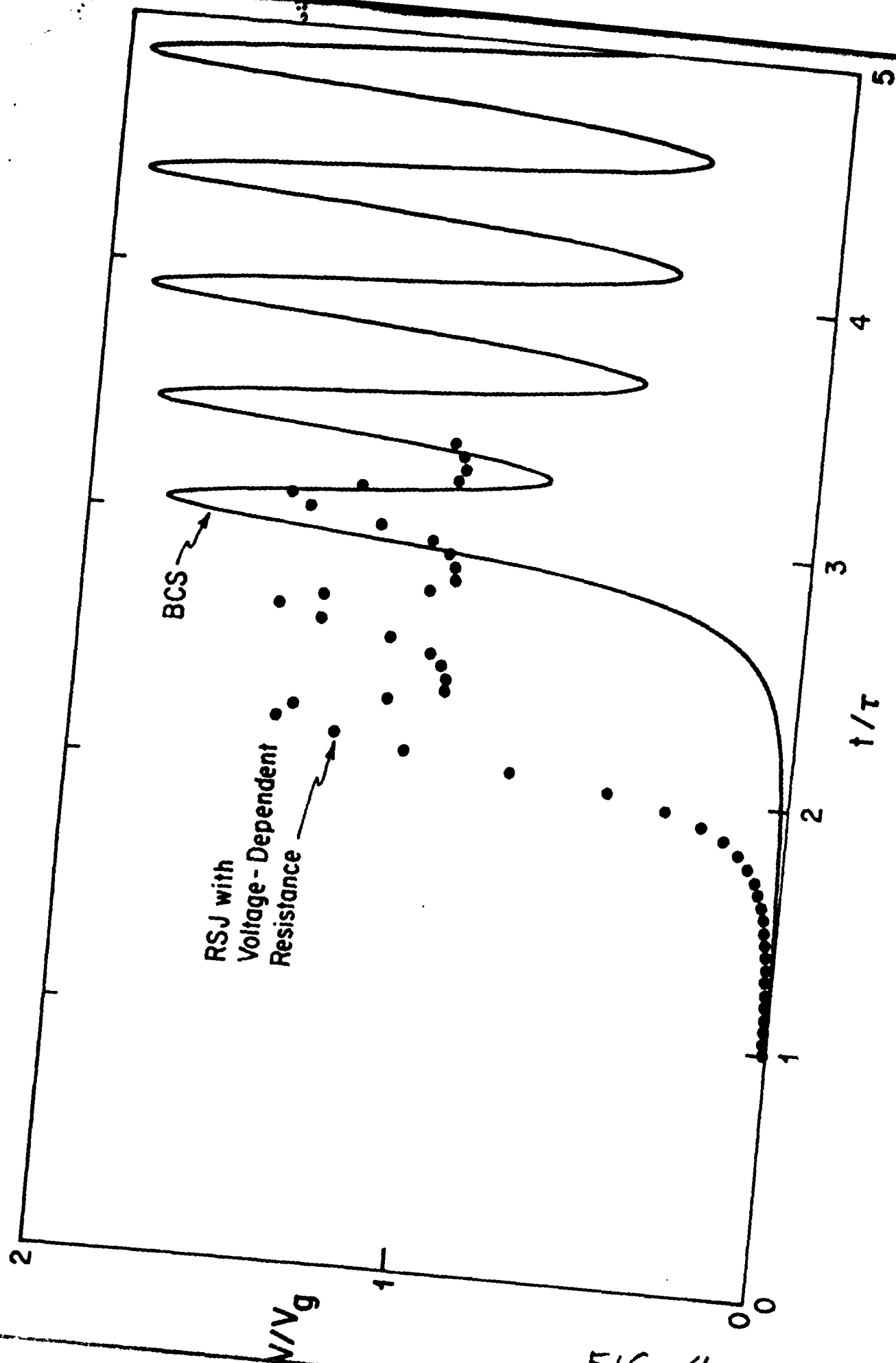peak until $t/\tau = 7.9$.

FIG. 1

Fig. 2

Fig. 3(a)

Fig. 3(b)

FIG. 4

Multiple magnetic flux entry into superconducting quantum-interference devices (SQUIDs): A general way of examining the cosφ conductance

Robert L. Peterson

Electromagnetic Technology Division, National Bureau of Standards, Boulder, Colorado 80303

Robert I. Gayley

Department of Physics, State University of New York at Buffalo, Amherst, New York 14260
(Received 13 February 1978)

A new type of experiment is proposed for obtaining information about the cosφ conductance of the Josephson effect. Based on measurement of fluxoid entry into a superconducting ring broken by a Josephson junction, the technique is to operate in the low-damping regime for which the voltage excursions associated with fluxoid entry are small. For this case, the constant voltage expression containing the cosφ conductance should be valid. It is shown that the erraticity associated with the low-damping regime has a predictable statistical pattern, which is rather insensitive to noise but quite sensitive to the cosφ term. A shunt resistance can be used to vary the average voltage. Statistics can be accumulated over a large number of similar loops, or over one or a few loops at slightly varying bath temperature between runs, or even over one loop at one temperature provided the noise at the junction has appropriate properties. Thus, the technique would appear to be capable of estimating the controversial coefficient of the cosφ term as a function of voltage and temperature for any type of junction for which low damping can be achieved.

I. INTRODUCTION

The observation of multiple magnetic fluxoid entry, or "quantum transitions," into superconducting quantum-interference devices (SQUIDs)—superconducting rings which are broken by Josephson junctions—has been reported in many articles, usually with a qualitative or semiquantitative discussion of the underlying reasons for the multiple fluxoid entry (see, e.g., Ref. 1). In a typical experiment, a magnetic field is applied in a direction normal to the plane of the ring. When the applied flux reaches a certain threshold value, many magnetic flux quanta will enter through the junction in rapid succession. No more fluxoids enter the ring until the external flux reaches a second threshold, whereupon another group enters, etc.

Some recent articles[2-5] have reported results of detailed simulations of this phenomenon, using simple models for the junction. Smith and Blackburn[2] have shown that for rings with "high" damping β and large values of $\gamma \equiv LI_c/\Phi_0$ (symbols are defined later), the number of flux quanta entering the loop as the external magnetic flux reaches threshold is a unique and predictable function of the SQUID parameters. However, at small damping the number entering was shown by Wang and Gayley[3] to become erratic (or more accurately, extremely sensitive to small changes in parameters). The latter authors[4] later inserted the cosφ conductance[6,7] into their simulations and showed that it can greatly affect the number of fluxoids entering the loop in the high-damping region. The measurement of the number of fluxoids entering

the ring thus could give useful information about the cosφ conductance, a question which is now very much unsettled.[7-15] However, Gayley and Wang[3] cautioned that the high rapidly varying voltages expected to develop during the flux entry might render invalid the starting point of the calculation, namely the constant-voltage assumption[6,7] which leads to the appearance of an explicit cosφ term. That this is probably true is shown later in the present paper, as well as possibly by a recent high-damping experiment[5] in which the measured flux entry did not agree at all with simulations, with or without the cosφ term (see also Ref. 2 in this regard).

In this paper we consider especially the "erratic" low-damping case in more detail, for several reasons. First, erratic behavior is commonly observed in loops[16-20] and elsewhere.[21,22] Second, as we show later, the significant voltage change occurs over a time interval much longer than the inherent response times (picoseconds) of superconducting materials, thus, validating the constant-voltage expression [Eq. (1)] in the computations. And, finally, it is evident that the cosφ term should have a marked influence on flux entry in the low-damping regime as well as at high damping.

In the absence of noise and for a particular choice of parameter values and initial conditions, there is of course, one value for the final flux in the loop. However, at low damping, a small change in parameter values or a pulse of noise can result in a large change in the final flux. In this paper we argue that in spite of this, meaningful measurements can in fact be made with such a system. For

a reasonable amount of noise and a reasonable range of parameter values, the final flux will be distributed in a predictable way over a small subset of values. Therefore, the statistical distribution of a series of trials can be predicted. Since the $\cos\phi$ term affects this distribution, the experiment should yield a value for the coefficient of this term. Further, since the maximum voltage developed is controllable by a shunt resistance, such an experiment offers the possibility of determining the $\cos\phi$ coefficient as a function of voltage, a type of experiment not yet attempted. Tunnel junctions are here implied, because the damping constant can readily be made small with them. However, the theory and technique presented here would apply to any type of junction for which low damping could be achieved.

Finally, in the Appendix, we show by a simple argument the source of an empirical formula deduced from the simulations,[2] relating the damping to γ for single fluxoid admission. We also present a more accurate simple expression valid to within 1% down to $\gamma \simeq 1$. Knowledge of this relationship is important because some Josephson devices based on flux counting could give misleading results if more than one fluxoid enters at a time.

II. BASICS

The circuit analyzed is that of the simple junction shunted by capacitance and a phase-dependent conductance, and connected to a superconducting loop of inductance L (see Fig. 1). The tunnel current $I(t)$ into the junction, indicated in Fig. 1, was first derived by Josephson[6] for a tunnel junction to be

$$I(t) = I_c \sin\phi + \sigma_0 V + \sigma_1 V \cos\phi , \qquad (1)$$

in which a constant voltage V across the junction was assumed. The coefficients I_c, $\sigma_0 \cong 1/R$, and σ_1 are voltage dependent. The ratio σ_1/σ_0 has been calculated by Poulsen[13] at several temperatures, from tunneling theory, and is indicated schemati-

FIG. 2. Schematic diagram illustrating the dependence of σ_1/σ_0 upon voltage (solid curve), according to tunneling theory. The shaded rectangle indicates the locations of experimental determinations of σ_1/σ_0 for tunnel, microbridge, and point contact junctions. A recent experiment (Ref. 15) carried out on tunnel junctions at several temperatures near the critical temperature, showing both signs for σ_1/σ_0, but opposite to that expected from tunneling theory, is not shown.

cally in Fig. 2. The rectangle in Fig. 2 also indicates, with one recent exception,[15] the results of experiments designed to measure σ_1/σ_0, for tunnel, microbridge, and point-contact junctions. The vertical dimension of the rectangle is meant to suggest the error bars associated with most of the experiments. As is seen, the experiments tend to agree with each other. The results have a sign opposite to that predicted from tunneling theory, but are in approximate agreement with Landau-Ginsburg theory.[7,12] A recently published experiment[15] on tunnel junctions at temperatures very close to the critical temperature shows, however, a sign change as a function of temperature.

When an external magnetic field is applied to the loop of Fig. 1, the differential equation describing the circuit becomes

$$\frac{d^2\phi}{dt_1^2} + \beta\frac{d\phi}{dt_1}\left(1 + \frac{\sigma_1}{\sigma_0}\cos\phi\right) + 2\pi\gamma\sin\phi + \phi = \phi_x , \qquad (2)$$

where $t_1 = t/\sqrt{LC}$, $\beta = \sqrt{LC}/RC$, $\gamma = LI_c/\Phi_0$, I_c is the junction critical current (here assumed unaffected by the magnetic field which would typically be $\leq 10^{-6}$T $= 10^{-2}$G), ϕ is the superconducting phase difference across the junction, ϕ_x is the applied magnetic flux in units of $\Phi_0/2\pi$, and $\Phi_0 = 2.068 \times 10^{-15}$ Vs is the flux quantum. I_c, σ_0, and σ_1 are taken to be constants in our simulations. The resistance R is the quasiparticle tunneling resistance combined with any shunt resistance that may be present. In an experiment the resistance will be taken from the dc current-voltage characteristic
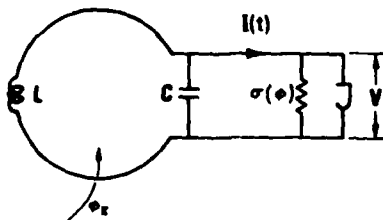

FIG. 1. Circuit used in the simulations of this paper. The three elements on the right comprise the Josephson junction. The tunnel current $I(t)$, as shown after the capacitance, is given in Eq. (1).
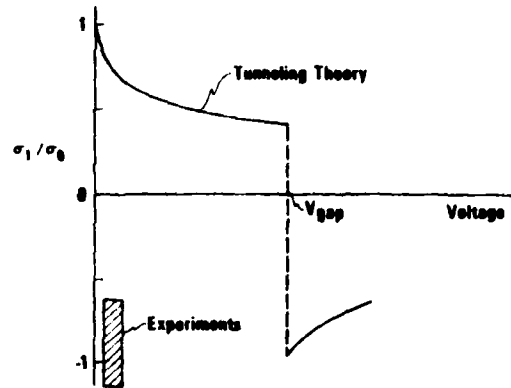
of the junction. In our calculations, we suppose that some average R is used, but it would be a simple matter to use the measured voltage-dependent resistance if this seemed desirable. The average voltage may be appreciably less than the gap voltage, so the tunneling resistance may be much larger than the normal state resistance of the junction. A shunt resistor may be inserted to obtain the desired value of β or to adjust the value of the average voltage.

Most of the remaining discussion in this section repeats material published earlier.[2,3] We feel it desirable to include it, however, because of the important insights provided by the potential-well picture. Note that the present ϕ and ϕ_x are equal to the earlier[2,3] Φ and Φ_x multiplied by 2π.

When ϕ_x is changing adiabatically, Eq. (2) can be cast into the intuitively appealing form

$$\frac{d}{dt_1}(T+\mathcal{V}) = -\beta\left(1+\frac{\sigma_1}{\sigma_0}\cos\phi\right)\left(\frac{d\phi}{dt_1}\right)^2, \tag{3}$$

where the "kinetic energy" T is $\frac{1}{2}(d\phi/dt_1)^2$, and the "potential energy" $\mathcal{V}$ is

$$\mathcal{V} = \tfrac{1}{2}(\phi-\phi_x) - 2\pi\gamma\cos\phi. \tag{4}$$

The term on the right-hand side of Eq. (3) represents viscous drag modulated by the $\cos\phi$ term.

The state of the system may be visualized as a particle moving along the potential $\mathcal{V}$ (see Fig. 3). As the field is raised slowly from zero, the particle stays at the bottom of the local well near $\phi = 0$ until ϕ_x is large enough that the local minimum is now an inflection point (and also the local maximum), whereafter the particle begins to "slide" until stopped by the damping.

The extrema of $\mathcal{V}$ are given by

$$\frac{\partial\mathcal{V}}{\partial\phi} = 0 = \phi + 2\pi\gamma\sin\phi - \phi_x, \tag{5}$$

and the inflection points by

$$\frac{\partial^2\mathcal{V}}{\partial\phi^2} = 0 = 1 + 2\pi\gamma\cos\phi. \tag{6}$$

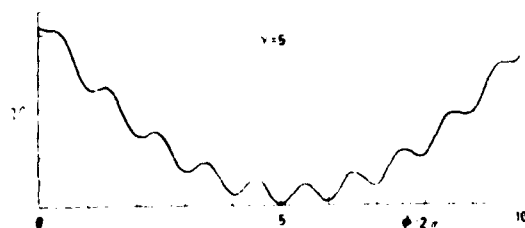The solution of Eq. (6) for ϕ, substituted into Eq.

FIG. 3. "Potential" $\mathcal{V}$ of Eq. (4) plotted for $\gamma=5$ and ϕ_x 5.253 $\times 2\pi$.

(5), specifies what ϕ_x must be at the beginning of the motion of the particle. One finds for the "break-in" value of the externally applied normalized flux

$$\phi_x = \cos^{-1}\left(-\frac{1}{2\pi\gamma}\right) + \left(4\pi^2\gamma^2 - 1\right)^{1/2}$$

$$= 2\pi\gamma + \frac{\pi}{2} + \frac{1}{4\pi\gamma} + O(\gamma^{-2}), \tag{7}$$

and for the starting inflection point ϕ_i,

$$\phi_i = \cos^{-1}(-1/2\pi\gamma) = \tfrac{1}{2}\pi + 1/2\pi\gamma + O(\gamma^{-2}). \tag{8}$$

The next inflection point at positive slope is of course at $2\pi + \phi_i$. Its adjacent mimimum and maximum are at $\frac{5}{2}\pi \pm (2/\gamma)^{1/2} + O(\gamma^{-1})$. The intermediate inflection point is at $2\pi - \phi_i = \frac{3}{2}\pi - \frac{1}{2}\pi\gamma + O(\gamma^{-2})$. The latter quantities will be used in the Appendix, where we consider threshold damping for single fluxoid admission.

Figure 3 shows a plot of the potential $\mathcal{V}$, Eq. (4), for $\gamma = 5$, and ϕ_x equal to its "break-in" value of $2\pi \times 5.253$. Note that there are about γ local wells between the starting inflection point and the bottom of the "bowl," or overall potential. Thus, if the particle stops at the bottom, γ fluxoids have been admitted into the loop. We shall use the terminology "high damping" and "low damping" to mean, respectively, the cases in which the particle stops before reaching the bottom, or sweeps past it.

III. BEHAVIOR AT LOW DAMPING, WITHOUT NOISE

As mentioned earlier, when Gayley and Wang[4] introduced the $\cos\phi$ term into their simulations at high damping and found a large effect, they cautioned that large voltage excursions might be expected which would possibly invalidate their starting point, Eq. (1). That this is true is shown in Fig. 4 for $\gamma = 100$ and $\beta = 12$, a typical high-damp-
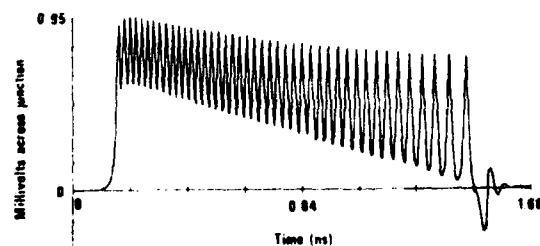

FIG. 4. Typical high-damping case: $\beta = 12$, $\gamma = 100$. Circuit parameters which give these values of β and γ are, for example, $L = 2000$ pH, $C = 14$ pF, $I_c = 0.1$ mA, $R = 1\ \Omega$, $\sigma_1 = 0$. The time and voltage scales are based on these values. The gap voltage is not determined by the RI_c product, since R is not necessarily the junction normal-state resistance.

ing case. The voltage excursions approach 100% of the maximum voltage developed. Note that there is an infinitude of ways of choosing L, C, R, and I_c for given γ and β. For the values indicated in the caption, each voltage excursion takes place in about 30 ps. After fluxoid entry begins, some 43 fluxoids enter the loop in about 1 ns. Figure 4 can also be thought of as particle velocity as a function of time. The particle is trapped 0.43 of the way to the bottom of the bowl, whereupon it undergoes damped oscillations (the plasma oscillations) about the bottom of the local well.

The low-damping regime, however, is quite different. Here the voltage excursions are typically very small, and only the voltage envelope is important. Figure 5 illustrates a moderate damping case, with $\gamma = 484$ and $\beta = 1.77$. Even on a greatly expanded scale (not shown) the voltage excursions are scarcely discernible until the particle is nearly trapped, and even then the amplitudes are very small. For the typical circuit parameters used in Fig. 5, the voltage envelope, corresponding to the entry of about 480 fluxoids, develops over a time of about 3 ns, much longer than the picosecond response times of typical superconducting materials. The junction will thus readily follow this adiabatically varying voltage, and Eq. (1) should be a valid basis for simulations. An accurate calculation would incorporate the voltage dependence of σ_1/σ_0, but since this is "unknown"—this is what the experiment is all about—we treat it as a constant; the experiment then would determine σ_1/σ_0 as a function of the average voltage developed during flux entry. By means of a shunt resistance, the latter can be varied from values comparable to the gap voltage to much smaller values. In Fig. 5, for example, suppose that the gap voltage is 2 mV. Then the resistance of 2 Ω implies use of a shunt resistance only slightly greater than 2 Ω, since with $I_c - 0.4$ mA the normal junction resistance would be about 8 Ω.

The resistance on the low-voltage portion of the I-V curve actually being sampled would be considerably greater. As is seen, the average voltage developed during the flux entry is about 0.2 mV, or 10% of the assumed gap voltage.

A complicating effect occurs in the low-damping regime, however. Wang and Gayley[3] showed that the final state of the system seems to be erratic. Actually, the final state is a very sensitive but predictable function of the system parameters. An example is shown in Fig. 6 for $\beta = 1.20$, $\sigma_1 = \sigma_0$, and γ in the neighborhood of 1000. Here, there are two preferred final states, one near a final flux number of 1100 (the particle sweeps past the bottom of the bowl and is trapped about 10% up on the opposite wall), and the other near 1000 (the particle does not get trapped on the opposite wall, but falls back to near the bottom). These fluxoid numbers are consistent with the "approximate theoretical maximum and minimum" computed from Eq. (1) of Wang and Gayley.[3] Guéret[23] has also found two final states in a related calculation. For yet lower values of damping, there can be more than two possible final states.

For a damping constant near 1.2 and γ near 1000, the final fluxoid number for $\sigma_1 = +\sigma_0$ in, for example, the upper state differs by only a few from the upper state number for $\sigma_1 = -\sigma_0$. Thus, counting of fluxoids would have to be accurate within about 1% in this example, in order to determine a value for σ_1/σ_0 with error bars less than ±1. Although this may be possible, there is a much more important reason why fluxoid counting from a single measurement would be inadequate for examining the $\cos\phi$ term in low-damping loops. As we see from Fig. 6, it is not likely that we could know the γ of a given loop to sufficient precision to predict whether the final fluxoid number would be, for example, 1000 or 1100. Even if we knew γ accurate-
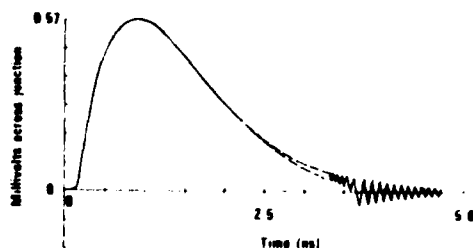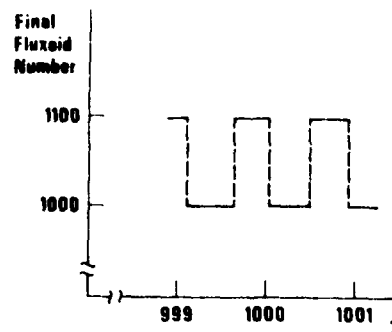

FIG. 5. Moderately low-damping case: $\beta = 1.77$, $\gamma = 484$. Circuit parameters, which determine the time and voltage scales, are: $L = 2500$ pH, $C = 200$ pF, $I_c = 0.4$ mA, $R = 2\ \Omega$, $\sigma_1 = 0$. The dashed lines indicate the voltage extrema.

FIG. 6. Final flux values in a superconducting loop with damping constant of 1.20, $\sigma_1 = \sigma_0$, and γ near 1000. Two states are selected by the system in an almost periodic fashion.

ly on one run, its value on a subsequent run would be slightly different if the bath temperature changed slightly. Thus, what would be obtained on a series of runs would be a statistical distribution over the possible final states.

We have observed that the "occupation numbers" of the final states are quite sensitive to the $\cos\phi$ term, yet insensitive to noise. That is, the fraction of the cases in which the system will end in a given preferred final state is sensitive to the value of σ_1/σ_0, and this fraction is readily determined from the simulations by varying γ in small increments. Thus, instead of having to count fluxoids with great precision, one has the attractive alternative of accumulating statistics, using relatively crude fluxoid counting. In such a procedure, one could fabricate a series of superconducting rings with closely similar values of γ. The individual values would presumably be distributed somewhat randomly within a small range, and the results of the flux measurements would be a statistical distribution of values among the preferred final states.

Rather than making measurements on a large number of similar loops, one would probably prefer to make repeated measurements on one or a few loops, deliberately varying the bath temperature slightly between measurements, for example, a few millidegrees. Since γ is proportional to I_c, which in turn is proportional to the temperature-dependent energy gap, this procedure would seem to be a convenient method for varying γ in small steps. Still another procedure (here anticipating the results of Sec. IV) might be to make repeated measurements on one or a few junctions at a "fixed" temperature, allowing the noise at the junction to be the statistical generator. As we shall see in Sec. IV, the noise parameters would have to fall in a certain range.

Table I shows the results of a ratio analysis at $\beta = 1.18$, 1.20, and 1.22, which is a reasonable range of uncertainty for this parameter. The Table entries show the percentage of the total number of possible times that the flux entry will be found in the upper of the two final states; they are determined by incrementing γ in very small steps, and are accurate to ± 0.1 (for the noise-free entries). The difference of more than a factor of 2 between the results at $\sigma_1 \sigma_0 = +1$ and -1 should make the distinction between these values readily discernible. The ultimate accuracy of the determination of σ_1/σ_0 will depend principally upon the amount of statistics accumulated. The effects of noise are discussed in Sec. IV.

There are of course other values of β and γ which may be appropriate. We selected the range displayed in Table I because just two well-separated

TABLE I. The entries in the σ_1 columns are the percentage of occurrences for which the final flux entry into the superconducting loop is in the high-flux state (about 1100 in this case). Values of γ near 1000 are used, with damping values β as shown. The last row indicates the results of noise simulations at a noise frequency of $1000/\sqrt{LC}$ and a noise amplitude of $0.1\phi_x$. Some 228 simulations using different sets of (pseudo) random numbers are used for each value of σ_1 in the noise simulations. The uncertainties indicated correspond to one standard deviation (Ref. 25).

γ	$\sigma_1 = +\sigma_0$	$\sigma_1 = 0$	$\sigma_1 = -\sigma_0$	Noise amplitude
1.18	55.8	27.7	16.5	0
1.20	40.6	30.0	18.1	0
1.22	43.6	32.4	19.8	0
1.20	43±3.3	29±3.6	17±2.5	$0.1\phi_x$

final states occur. Lower damping might result in, for example, three final states, two of which would likely be fairly close to each other, and possibly confuse the results. However, this is not necessarily so, because one might simply examine the well-separated state, unless its percentage occupancy is so low that adequate accumulation of statistics becomes difficult.

IV EFFECTS OF NOISE

It is important to understand the effects of noise on the results of Sec. III. Noise may be pictured as a rocking of the "bowl," representing the potential energy v, about its bottom. That is, from Eq. (4), the variation of the potential due to a variation $\delta\phi_x$ in ϕ_x is

$$\delta v = (\phi_1 - \phi)\delta\phi_x. \tag{9}$$

Thus, one might anticipate that noise would tend to make the flux entry more regular—the particle tends to get shaken toward the bottom of the bowl. For a particle trapped high on the wall of the bowl, which can occur only for very low damping, noise can fairly easily displace the particle from its relatively shallow local well. But for moderately low damping, in which the particle is trapped, for example, 10% above the bottom of the bowl, noise of "ordinary" amplitude will not displace the particle once the particle has settled down, which occurs after several plasma oscillation periods. One should also note that in addition to tending to prevent trapping in a certain well, noise can also promote trapping in a well in which the particle would not remain in the noise-free case. There is a strong symmetry in these two cases, which our simulations bear out.

Noise enters primarily through ϕ_x—even Johnson noise in the junction or shunt resistance[24] can be

lumped into ϕ_x. A "second-order" effect would lie in the variations of γ because of variations in I_c, e.g., because ϕ_x is noisy, but this can surely be ignored. Thermal fluctuations could also affect I_c through the energy gap, but both the amplitude and frequency would be too low to be of significance for temperatures not too close to T_c.

We have examined the effects of noise by adding to ϕ_1 a suitably distributed (pseudo)random number at each new time increment in the computation (or at some multiple thereof, thereby varying the noise frequency, or spectrum). Noise levels (standard deviations) up to 10% of ϕ_1 have been used.

It is evident that the "erraticity" at low damping will be dependent upon noise frequency. If the particle has not had time to settle to the bottom of a local well, a pulse of noise has a fair probability of kicking the particle out. Thus, the natural frequency against which to compare noise frequency is the plasma frequency, which is the frequency of the motion of the particle in a local well. This is readily obtained from Eq. (2) by setting $\phi = 2\pi n + \phi'$ where $|\phi'| \ll 1$ and n is an integer. The homogeneous solution to the equation thus linearized (and here dropping the "$\cos\phi$ term") is $\exp(p t_1)$ where

$$p = -\tfrac{1}{2}\beta \pm \left[\beta^2 - 4(1 + 2\pi\gamma)\right]^{1/2}. \tag{10}$$

Since β^2 is less than about 9γ for multiple flux entry (see the Appendix), this is an underdamped case. Further, if $\beta^2 \ll 8\pi\gamma$, which is the ordinary case for low damping, the angular plasma frequency ω_p is just $(8\pi\gamma)^{1/2}$ in t_1 space, or $(8\pi\gamma/LC)^{1/2}$ in real time. The damping time is $2/\beta \gtrsim \tfrac{1}{3}\gamma^{1/2}$, the inequality being the condition for multiple transitions, as above. Thus, the damping time is greater than the plasma period $2/(8\gamma/\pi)^{1/2}$, and the particle will always make several swings through the bottom of a local well before coming to rest.

The plasma period has a significance beyond that of a trapped particle: a particle traveling slowly, but not quite slowly enough to be trapped, clearly will require about one-half the plasma period in traveling from one local maximum to the next. Thus, we can easily estimate the time required, or the number of noise pulses occuring, when the particle moves from a fluxoid number of, for example, 1100 to 1000, to use the example of Sec. III.

There are two effects of noise which must be considered. (i) By how much does noise produce scatter about the preferred final states, and are the mean values shifted from the noise-free case? (ii) By how much does noise affect the *ratios* of the "occupation numbers" in the (now spread-out) final states? We anticipate that the preferred experimental procedure would be that of determining
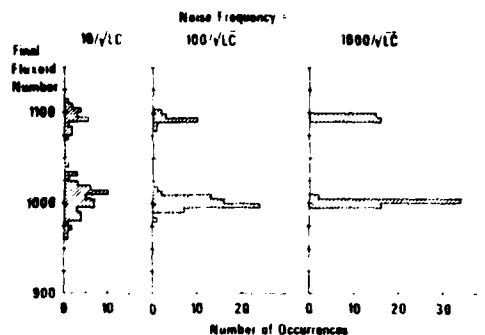

FIG. 7. Histograms showing how different noise frequencies affect the final flux values in a superconducting loop. Noise amplitude $= 0.05\,\phi_x$; $\beta = 1.20$; $\sigma_1 = 0$; nine values of γ in the range from 999.0 to 1001.7. About 80 runs were made at each noise frequency.

the ratios. Thus, question (i) is not important unless the scatter is so great that the clusters overlap.

That the mean values of the final states should not be materially affected by noise, as seen in Fig. 7, is intuitive: The preferred states are determined by the values of β and γ. If, for example, a small change of γ changes the trapping point from the upper to the lower of two preferred states, by the same reasoning a noise kick on the trapped particle near the extreme of its plasma oscillation swing can eject the particle and cause it to seek the lower preferred state.

Scattering obviously increases with increasing noise amplitude. The example of Fig. 7 shows no overlap between clusters even at the relatively large noise amplitude of $0.05\phi_1$. The influence of noise frequency upon the scatter is, however, not so easy to understand, and certainly not easy to explain in a few words. Since the question is not important in the present context, we shall offer only the following: When the noise frequency is low, the last noise pulse before trapping (or nontrapping) is important and may cause trapping in an "abnormal" state, thus, causing scatter. When the noise frequency is high, however, there is a great amount of self-cancellation of the noise, and the scatter is smaller. Our simulations do show that for noise frequencies ω_x less than ω_p, there is a good bit of scatter about the final states, whereas for $\omega_x \gg \omega_p$, the clustering is quite narrow. Figure 7 illustrates this for three values of noise frequency: $10\sqrt{LC}$, $100\sqrt{LC}$, and $1000\sqrt{LC}$. These are to be compared to the plasma frequency $\sqrt{2\pi}\sqrt{LC} \sim 25\sqrt{LC}$ for $\gamma \sim 1000$.

The important question is number (ii) above. One expects that the occupation number ratios will not be greatly affected by "reasonable" noise

amplitudes since the trapping and nontrapping situations should be affected rather symmetrically by the noise. All the simulations we have made bear this out. Table I illustrates this for γ near 1000 and β near 1.2, at the very large noise amplitude of 0.1 ϕ_x and a noise frequency of $1000/\sqrt{LC}$. The 228 calculations made for each value of σ_1 result in an uncertainty in the listed percentages as shown by the indicated standard deviations.[25] Calculations at smaller noise amplitudes have also been made, and also show the insensitivity of the percentages to noise.

Finally, our simulations with noise show that the percentages are not biased by choice of γ, for a given β. For example, if we consider only those values of γ, within the range 999–1001, for which the final state would be the lower of the two possible states in the noise-free case, we find the same percentages as given in Table I to within our statistical significance. Thus, an experiment making repeated runs on a single junction, allowing the noise at the junction to generate the statistics, may be an acceptable technique. Of course, the noise amplitude has to be large enough to be effective, but not so large as to produce chaotic results. Our simulations have shown that quite a broad range of noise amplitude is acceptable. A noise frequency comparable to or larger than the plasma frequency would also be desirable.

V. CONCLUSIONS

We conclude that it should be possible to derive useful information about the $\cos\phi$ conductance by measurement of fluxoid entry into a superconducting loop at low damping. Low damping ensures that the basic equation containing the $\cos\phi$ term is a valid basis for this type of experiment.

The procedure described in this paper should greatly improve our knowledge of σ_1 at low voltage. Moreover, by use of a shunt resistance, the average voltage developed during flux entry can be controlled, and thus σ_1/σ_0 can be estimated as a function of voltage, a dependence which has not been measured to date. Since tunneling theory predicts a large discontinuity in σ_1/σ_0 at the gap voltage, with a sign reversal, measurements near such voltage would be particularly exciting.

The temperature dependence of σ_1/σ_0 could also be obtained, obviously, by varying the bath temperature. It would be interesting to compare such results with those recently obtained.[15]

Noise is not likely to be an obscuring factor, according to our calculations and may be desirable in accumulating statistics.

Finally, provided low damping can be achieved, the experiment can be performed with any type of Josephson junction. This could be very interesting because to date each type of junction—tunnel, microbridge, or point contact—has used an entirely different experimental method for examining the $\cos\phi$ conductance.

Measurement of fluxoid entry at *high* damping can also be made, but as Gayley and Wang[4] pointed out, a theory allowing for a dynamic voltage[26] should then be used to calculate the expected fluxoid number. Since the theory for large rapidly varying voltage would not have an explicit $\cos\phi$ term, one could not then speak of determining the value of σ_1/σ_0, but only of confirming or denying the validity of the complete theory.

APPENDIX

In this Appendix we consider the threshold damping for single fluxoid entry, in order to show the source of a relation deduced empirically from earlier simulations.[2,5] We also develop a more accurate expression valid over a larger range of γ.

To examine the threshold damping in question, we ask: What must be the value β_t of the damping constant β in order that the particle not slide beyond the first maximum of the potential $\mathcal{U}$ at $\frac{1}{2}\pi + (2/\gamma)^{1/2}$? (The positions of the first few extrema and inflection points of $\mathcal{U}$ were obtained in Sec. II.) The relation deduced empirically[2,5] for γ in the region above 100 is $\beta_t = 3.0\gamma^{1/2}$. To show the source of this relation we use the following simple argument. First, we observe that for $\gamma \gg 1$, as illustrated in Fig. 8 for $\gamma = 200$, the potential energy curve is quite steplike initially, rather than having pronounced minima and maxima. This suggests approximating the potential by the piecewise linear portions shown in Fig. 8. We draw a horizontal line through ϕ_{min} and a straight line with the correct negative slope of $-4\pi\gamma$ through the inflection point near $\phi = \frac{1}{2}\pi$. One can easily show,
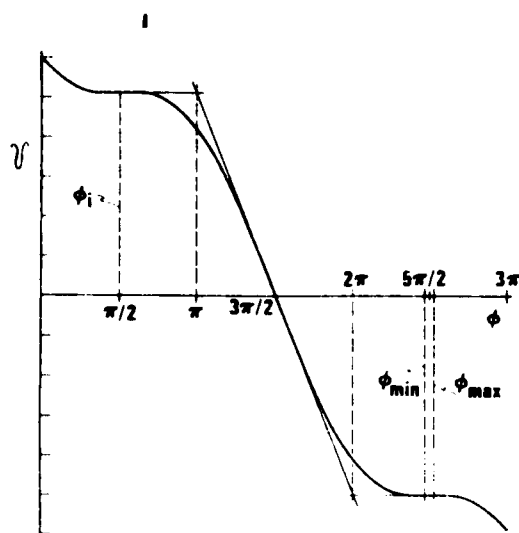
FIG. 8. First portion of the potential $\mathcal{V}$ for $\gamma = 200$ and $\Phi_i = 2\pi \times 200.250$, together with the piecewise linear portions used to approximate $\mathcal{V}$ in this region. The vertical scale is arbitrary.

once β_1 is estimated, that the particle sliding down the linear slope will nearly have its terminal velocity

$$\frac{d\phi}{dt_1}\Big|_{terminal} = \frac{4\pi\gamma}{\beta} ,\tag{A1}$$

when the horizontal portion is reached. On a horizontal line, the particle travels a distance equal to its initial velocity divided by the damping constant; that is,

$$\phi_{stop} = \phi_{start} + \frac{1}{\beta}\frac{d\phi}{dt_1}\Big|_{terminal} .\tag{A2}$$

Setting the asymptote ϕ_{stop} equal to $\frac{5}{2}\pi$, and ϕ_{start} equal to 2π [the intersection of the two straight lines is at $2\pi + O(\gamma^{-1})$], requires $\beta_1 = (2/\pi) \times (d\phi/dt_1)|_{terminal}$, which with Eq. (A1) gives

$$\beta_1 = (8\gamma)^{1/2} ,\tag{A3}$$

which has the observed square-root behavior. Note that $8^{1/2} = 2.83$. Note also that if in Eq. (A2) the asymptote is refined to $\frac{5}{2}\pi + (2/\gamma)^{1/2}$ then Eq. (A3) becomes

$$\beta_1 = (8\gamma)^{1/2} - 4/\pi ;\tag{A4}$$

that is, an offset is predicted. We have made a computer study of β_1 vs γ down to values for which β_1 vanishes. The expression

$$\beta_1 \approx 2.99\gamma^{1/2} - 2.53 ,\tag{A5}$$

is accurate to within 1% for all values of γ above unity. For $\gamma < 1$, β_1 dips slightly below this line and falls to zero at $\gamma_{min} = 0.733$. At this value, the second maximum of $\mathcal{V}$ has risen to the level of the starting point, so that even at zero damping, not more than one fluxoid can enter the loop. γ_{min} is the solution of

$$2\pi\gamma \cos(4\pi^2\gamma^2 - 1)^{1/2} = -1 ,\tag{A6}$$

which results from requiring that $\phi + 2\pi\gamma \sin\phi$ have the same value at ϕ_i as at $4\pi - \phi_i$.

Knowledge of threshold damping is important because any Josephson device acting as a flux counter in some measurement process could give quite misleading results if more than one fluxoid would enter at a time. For example, in the analog-to-digital conversion of a continuous signal which causes fluxoid entry or expulsion from a superconducting loop, the reconstructed signal could be quite distorted if this occurred.[27]

[1] D. B. Sullivan, R. L. Peterson, V. E. Kose, and J. E. Zimmerman, J. Appl. Phys. 41, 4865 (1970).

[2] H. J. T. Smith and J. A. Blackburn, Phys. Rev. B 12, 940 (1975).

[3] T. C. Wang and R.I. Gayley, Phys. Rev. B 15, 3401 (1977).

[4] R. I. Gayley and T. C. Wang, Phys. Rev. B 16, 3270 (1977).

[5] J. A. Blackburn, H. J. T. Smith, and V. Keith, Phys. Rev. B 15, 4211 (1977).

[6] B. D Josephson, Phys. Lett. 1, 251 (1962); Rev. Mod. Phys. 36, 210 (1964); Adv. Phys. 14, 419 (1965).

[7] H. Højgaard Jensen and P. E. Lindelof, J. Low Temp. Phys. 23, 469 (1976).

[8] D. N. Langenberg, Rev. Phys. Appl. 9, 35 (1974).

[9] N. F. Pedersen, R. F. Finnegan, and D. N. Langenberg, Phys. Rev. B 6, 4151 (1972).

[10] C. M. Falco, W. H. Parker, and S. E. Trullinger, Phys. Rev. Lett. 31, 933 (1973).

[11] M. Nisenoff and S. Wolf, Phys. Rev. B 12, 1712 (1975).

[12] D. A. Vincent and B. S. Deaver, Jr., Phys. Rev. Lett. 32, 212 (1974); R. Rifkin, D. A. Vincent, and B. S. Deaver, Jr., J. Appl. Phys. 47, 2645 (1976); B. S. Deaver, Jr., R. Rifkin, and R. D. Sandell, J. Low Temp. Phys. 25, 409 (1976).

[13] U. K. Poulsen, Rev. Phys. Appl. 9, 41 (1974).

[14] R. E. Harris, Phys. Rev. B 10, 84 (1974).

[15] O. H. Soerensen, J. Mygind, and N. F. Pedersen, Phys. Rev. Lett. 39, 1018 (1977).

[16] A. M. Goldman, P. J. Kriesman, and D. J. Scalapino, Phys. Rev. Lett. 15, 495 (1965).

[17] R. C. Jaklevic, J. Lambe, J. E. Mercereau, and A. H. Silver, Phys. Rev. 140, A1628 (1965).

[18] J. Wilson and R. I. Gayley, Solid State Commun. 11, 1183 (1972).

[19] T. A. Fulton, L. N. Dunkleberger, and R. C. Dynes, Phys. Rev. B 6, 855 (1972).

[20] N. H. Zappe and K. R. Grebe, J. Appl. Phys. 44, 865

(1973).

[21] T. A. Fulton and R. C. Dynes, Solid State Commun. 9, 1069 (1971).

[22] T. A. Fulton, Appl. Phys. Lett. 19, 311 (1971)

[23] P. Guéret, J. Appl. Phys. 44, 1771 (1973).

[24] R. L. Peterson and D. G. McDonald, IEEE Trans. Mag. MAG-13, 887 (1977).

[25] The noise entries ($m \pm s$) are made as follows: the number of times the system ends in the high state, divided by the number of trials (228), and multiplied by 100, gives the main entry m. The percentage standard deviation s is determined by adopting the sample mean ($m/100$) as true mean, computing the standard deviation of each trial about this mean, multiplying by $\sqrt{228}$ to determine the sample standard deviation, and finally multiplying by 100/228 to obtain s.

[26] N. R. Werthamer, Phys. Rev. 147, 255 (1966).

[27] R. L. Peterson and D. B. Sullivan (unpublished).